Science Bulletin 64 (2019) 998–1010

Contents lists available at ScienceDirect

Science Bulletin

journal homepage: www.elsevier.com/locate/scib

Article

ASAF: altered spontaneous activity fingerprinting in Alzheimer's disease based on multisite fMRI

Jiachen Li [a,1], Dan Jin [b,c,1], Ang Li [b,c], Bing Liu [b,c,d], Chengyuan Song [e], Pan Wang [f,g], Dawei Wang [h], Kaibin Xu [b], Hongwei Yang [i], Hongxiang Yao [j], Bo Zhou [g], Alexandre Bejanin [k], Gael Chetelat [k], Tong Han [l], Jie Lu [i], Qing Wang [h], Chunshui Yu [m], Xinqing Zhang [a], Yuying Zhou [f], Xi Zhang [g], Tianzi Jiang [b,c,d], Yong Liu [b,c,d,*], Ying Han [a,n,o,p,*]

[a] Department of Neurology, Xuanwu Hospital of Capital Medical University, Beijing 100053, China
[b] Brainnetome Center & National Laboratory of Pattern Recognition, Institute of Automation, Chinese Academy of Sciences, Beijing 100190, China
[c] School of Artificial Intelligence, University of Chinese Academy of Sciences, Beijing 100049, China
[d] Center for Excellence in Brain Science and Intelligence Technology, Institute of Automation, Chinese Academy of Sciences, Beijing 100190, China
[e] Department of Neurology, Qilu Hospital of Shandong University, Ji'nan 250012, China
[f] Department of Neurology, Tianjin Huanhu Hospital, Tianjin 300350, China
[g] Institute of Geriatrics and Gerontology, Chinese PLA General Hospital, Beijing 100853, China
[h] Department of Radiology, Qilu Hospital, Ji'nan 250012, China
[i] Department of Radiology, Xuanwu Hospital of Capital Medical University, Beijing 100053, China
[j] Department of Radiology, Chinese PLA General Hospital, Beijing 100853, China
[k] Université Normandie, Inserm, Université de Caen-Normandie, Inserm UMR-S U1237, GIP Cyceron, Caen 14000, France
[l] Department of Radiology, Tianjin Huanhu Hospital, Tianjin 300350, China
[m] Department of Radiology, Tianjin Medical University General Hospital, Tianjin 300052, China
[n] Center of Alzheimer's Disease, Beijing Institute for Brain Disorders, Beijing 100053, China
[o] Beijing Institute of Geriatrics, Beijing 100053, China
[p] National Clinical Research Center for Geriatric Disorders, Beijing 100053, China

ARTICLE INFO

Article history:
Received 16 November 2018
Received in revised form 22 March 2019
Accepted 25 March 2019
Available online 30 April 2019

Keywords:
Brain spontaneous activity
Multisite
Biomarkers
Leave-one-site-out cross-validation
Alzheimer's disease

ABSTRACT

Several monocentric studies have noted alterations in spontaneous brain activity in Alzheimer's disease (AD), although there is no consensus on the altered amplitude of low-frequency fluctuations in AD patients. The main aim of the present study was to identify a reliable and reproducible abnormal brain activity pattern in AD. The amplitude of local brain activity (AM), which can provide fast mapping of spontaneous brain activity across the whole brain, was evaluated based on multisite rs-fMRI data for 688 subjects (215 normal controls (NCs), 221 amnestic mild cognitive impairment (aMCI) 252 AD). Two-sample *t*-tests were used to detect group differences between AD patients and NCs from the same site. Differences in the AM maps were statistically analyzed via the Stouffer's meta-analysis. Consistent regions of lower spontaneous brain activity in the default mode network and increased activity in the bilateral hippocampus/parahippocampus, thalamus, caudate nucleus, orbital part of the middle frontal gyrus and left fusiform were observed in the AD patients compared with those in NCs. Significant correlations ($P < 0.05$, Bonferroni corrected) between the normalized amplitude index and Mini-Mental State Examination scores were found in the identified brain regions, which indicates that the altered brain activity was associated with cognitive decline in the patients. Multivariate analysis and leave-one-site-out cross-validation led to a 78.49% prediction accuracy for single-patient classification. The altered activity patterns of the identified brain regions were largely correlated with the FDG-PET results from another independent study. These results emphasized the impaired brain activity to provide a robust and reproducible imaging signature of AD.

1. Introduction

Alzheimer's disease (AD) is the main cause of dementia. Patients with AD present with initial memory disorder and

* Corresponding authors.
E-mail addresses: yliu@nlpr.ia.ac.cn (Y. Liu), hanying@xwh.ccmu.edu.cn (Y. Han).
[1] These authors contributed equally to this work.

https://doi.org/10.1016/j.scib.2019.04.034
2095-9273/

progressive cognitive impairment, namely, conversion of normal cognition to mild cognitive impairment (MCI) [1,2], that ultimately results in an inability of the aging population to work and carry out daily activities [3]. Furthermore, the burden of dementia is increasing rapidly worldwide [4,5]. The pathology of AD manifests with widespread accumulation of the amyloid-β (Aβ) and tau proteins, underlying hypometabolism and specific brain atrophy in regions of the temporal and parietal lobes [6–9]. The impairment caused by AD pathology is irreversible. Therefore, it is urgent to identify valid and reliable hallmarks of AD that can be used to predict the risk of AD dementia and provide the opportunity for early intervention (Fig. 1).

Neuroimaging has become a widely used technique for investigating the structural and activity patterns of the brain. According to a proposed biomarker model of AD [10], functional magnetic resonance imaging (fMRI) was used to identify predictors that may reflect clinical progression [11], such as the molecular deposition of AD pathology and synaptic dysfunction at the early stage of AD [12,13]. Although the neuroimaging community has traditionally focused on hypothesis-driven studies, resting-state fMRI (rs-fMRI) has recently been widely recognized as a powerful and easily applied tool that is acceptable for use in patients with dementia [12]. Notably, amplitude of low-frequency fluctuations (ALFF) [14] have been widely utilized to characterize spontaneous brain activity with the confirmation of objective cognitive performance [15] and even to discriminate AD patients from control subjects [16]. A previous study showed that a significant correlation exists between the amyloid load of the whole cerebral cortex and low fractional ALFF (fALFF) in AD patients [17]. However, evidence from the literature is more mixed across different imaging studies [18–27] (summarized in Table 1). Several studies have reported functional abnormalities of the default mode network (especially in the posterior cingulate cortex/precuneus (PCC/PCu)); nevertheless, these studies did not reach a consensus about whether AD patients exhibit increased [19,22,24,28] or decreased [25,29] activity in the hippocampus/parahippocampus compared with that in normal control (NC) subjects. Hence, across-sample reproducibility, regional specificity alterations, associations between spontaneous brain features, and clinical correlates of brain activity differences in AD remain largely unknown.

Although the irreproducibility of promising findings is not rare in neuroscience fields [30], the resting-state BOLD signal is a technically effective and reliable index for characterizing the intrinsic activity of the brain [31,32]. There is some consistency among

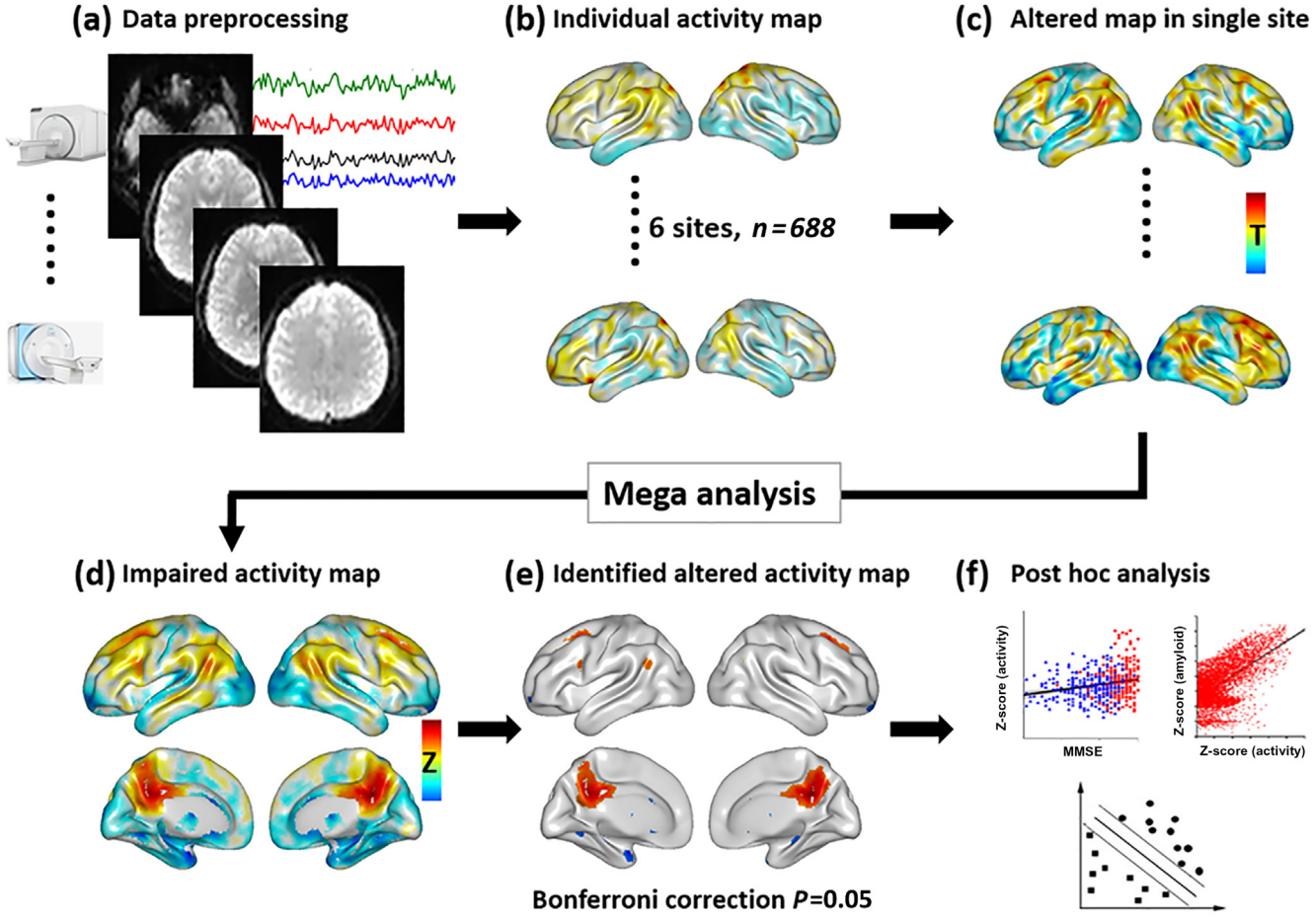

Fig. 1. Schematic of the data analysis pipeline. (a) Resting-state fMRI data were preprocessed in the following steps: slice timing, realignment, normalization, denoising, filtering and smoothing. (b) For each subject, the amplitude of local brain activity (AM) was calculated for each voxel. (c) For each center, a two-sample *t*-test was used to detect group differences between patients with AD and NC to identify the altered brain regions. (d) The statistical discrepancy diagrams were further analyzed with Stouffer's multisite analysis with the Liptak-Stouffer Z-score method (*P* values of six scanners were converted to one statistical Z-score). (e) Identify the brain regions with significantly altered brain activity at six sites ($P < 0.05$, Bonferroni corrected). (f) Correlations between the normalized amplitude index of the regions and cognitive ability were computed to evaluate the alteration of brain spontaneous activity associated with cognitive decline in the patient groups. Multivariate pattern analysis utilizing the SVM was conducted to classify the AD patients and normal controls based on brain activity patterns using leave-one-site-out cross-validation. The consensus features were used to identify the activity that contributed most to the classification. The correlations between the Z-scores of the present study and the Z-maps of FDG-PET results from previously published literature were also evaluated.

Table 1
Overview of large-scale whole brain functional network studies in MCI and AD based on fMRI data.[a]

Study	Methods	Subjects	*n*	Frequency (Hz)	Regions that showed increased brain activity in AD	Regions that showed decreased brain activity in AD
He et al. [18]	ALFF sMRI	Early stage of AD NC	14 14	0.01–0.10	Right cuneus	PCC/PCu
Wang et al. [19]	ALFF	AD aMCI NC	16 16 22	0.01–0.08	Bilateral HIP/PHIP, bilateral SMA, bilateral SFG, left FG, left ITG/STG and left PoCG	PCC/PCu, left OFG, left LN, right ALC
Dai et al. [28]	ALFF sMRI	Early stage of AD NC	16 22	0.01–0.10	Left HIP, bilateral FG, right ORBsup	Left PCG PCC
Song et al. [20]	ALFF sMRI	AD aMCI NC	35 18 21	0.01–0.08	None	PCC, left PCC, right PCu, bilateral PCu, left superior parietal lobule (5 regions chosen as ROIs)
Wen et al. [26]	ALFF	AD NC	15 16	0.01–0.10	None	MPFC, left IPC
Liu et al. [21]	AM	Severe AD Mild AD MCI NC	18 17 18 21	0.060–0.125	None	Bilateral PCC, bilateral PCu, bilateral middle temporal gyrus, bilateral angular gyrus
Liu et al. [22]	ALFF	AD NC	23 27	0.010–0.027	HIP/PHG, middle temporal gyrus, inferior temporal gyrus	Bilateral PCC/PCu, IPL, middle temporal gyrus, inferior temporal gyrus
Weiler et al. [23]	ALFF	AD aMCI NC	32 20 29	0.01–0.08	None	PCC
Liang et al. [24]	ALFF	AD Early MCI Late MCI NC	14 24 29 35	0.01–0.08	Right PHG	Thalamus, LG, bilateral PCC, bilateral PCu
Mascali et al. [27]	ALFF	AD aMCI NC	10 10 10	0.010–0.027; 0.027–0.073	None	None
Cha et al. [25]	ALFF	AD aMCI NC	37 34 62	0.009–0.080	None	Left PHIP, PCC
Wang et al. [29]	ALFF	APOE ε4 carriers at an early stage of AD Noncarriers at an early stage of AD	16 26	0.01–0.10	None	Left HIP

[a] Abbreviations: PCC = posterior cingulate cortex; PCu = precuneus; HIP = hippocampus; PHIP = parahippocampal gyrus; SMA = supplementary motor area; SFG = superior frontal gyrus; FG = fusiform gyrus; ITG = inferior temporal gyrus; STG = superior temporal gyrus; PoCG = postcentral gyrus; OFG = orbitofrontal gyrus; LN = lentiform nucleus; ALC = anterior lobe of the cerebellum; SFG_orb = orbital part of the superior frontal gyrus; MPFC = medial prefrontal cortex; IPC = inferior parietal cortex; IPL = inferior parietal lobe; LG = lingual gyrus; sMRI = structure MRI; NC = normal control; ROI = region of interest.

the reported differences in AD across studies; however, heterogeneous observations have been hampered by the small sample sizes used, variations in preprocessing methodologies, nonuniformity of data inclusion protocols, etc. The above studies based on a small sample size may not reflect the true effect [33] or subtle abnormalities between groups [34]. On the other hand, while preprocessing procedures can now be considered nearly standardized, the steps of the preprocessing pipeline vary from one procedure to another. Different data processing pipelines severely impact the main results among studies [35]. Furthermore, different data inclusion protocols might influence the results between studies; for example, some studies pooled mild cognitive impairment (MCI) and AD together as early-stage AD [18,28,29], which is a disadvantage for concluding a consistent pattern of ALFF in AD. Theoretically, meta-analysis is an effective method to identify replicable results from existing literature [36]. In fact, several excellent and timely studies have performed meta-analyses to identify consistent patterns in aberrant brain activity and have suggested that aMCI/AD is associated with widespread altered regional spontaneous brain activity in several important networks, such as the default mode network, salience network, visual network and episodic memory network [37–42].

The reliability and reproducibility of fMRI is a critical and fundamental issue for its clinical application [43,44]. Based on large sample sizes, ALFF showed good test-retest reliability from the voxelwise metrics throughout the entire brain [31,45,46], especially in the default mode network [31,47,48], which is vulnerable in AD. Meta-analyses that pool analyses of published results might be limited by variances in data processing and statistical thresholds across studies. In contrast, a mega-analysis (pooled analysis of raw data) across scanners can lead to more heterogeneity and novel scientific insights into the participant samples [49]. Therefore, a quantitative systemic analysis of the changes in brain activity based on raw data is highly warranted to delineate altered brain activity patterns and the underlying mechanisms in AD. The main aim of the present study was to identify a reliable and reproducible abnormal brain activity pattern in AD using a voxel-based approach by taking advantage of a thorough and detailed mega-analysis technique. Specifically, we sought to (1) identify changes in the brain activities of AD patients compared with those of normal controls (NCs), (2) evaluate the disease severity-associated alterations across patient groups that may reflect common and/or distinct neuropathological pathways, and (3) investigate whether brain activity could be used to differentiate AD patients from control participants.

2. Materials and methods

2.1. Participants

The study included 688 subjects (215 NCs, 221 MCI patients and 252 AD patients) that were analyzed using six different MRI scanners (PL_G and PL_S from Chinese PLA General Hospital; HH_Z

Table 2
Demographic and neuropsychological data of participants in the six datasets.[a]

Site	Groups	n = 688	Age	P	Sex (M/F)	P	MMSE	P
PL_S	NC	41	68.6 ± 6.7	0.75	19/22	0.75	28.5 ± 1.4	<0.0001
	MCI	34	69.5 ± 8.8		13/21		26.6 ± 2.5	
	AD	44	69.9 ± 8.9		20/24		17.3 ± 6.5	
PL_G	NC	21	68.6 ± 4.7	0.07	11/10	0.13	28.9 ± 1.1	<0.0001
	MCI	25	73.4 ± 7.9		12/13		27.0 ± 1.8	
	AD	24	72.8 ± 8.3		6/18		19.2 ± 4.6	
HH_Z	NC	24	65.5 ± 6.2	0.41	9/15	0.29	28.8 ± 1.2	<0.0001
	MCI	33	65.4 ± 8.3		10/23		25.9 ± 2.5	
	AD	37	67.7 ± 8.3		18/19		15.8 ± 5.5	
QL_W	NC	42	65.5 ± 6.8	0.23	12/30	0.20	28.4 ± 1.8	<0.0001
	MCI	16	66.1 ± 7.4		8/8		24.8 ± 1.2	
	AD	65	67.8 ± 7.1		28/37		19.8 ± 3.0	
XW_H	NC	66	66.5 ± 6.3	0.30	26/40	0.13	28.2 ± 2.2	<0.0001
	MCI	95	67.7 ± 9.9		48/47		24.1 ± 3.6	
	AD	47	69.1 ± 8.5		16/31		16.7 ± 6.4	
XW_Z	NC	21	65.0 ± 8.2	0.11	7/14	0.35	28.5 ± 1.4	<0.0001
	MCI	18	70.2 ± 7.9		10/8		21.9 ± 5.0	
	AD	35	65.8 ± 8.3		17/18		10.1 ± 6.7	

[a] *Chi*-squared tests were used for gender comparisons; one-way ANOVA was performed for age and MMSE comparisons. Detailed information about the data can be found in the supplemental material. Abbreviation: MMSE = Mini-Mental State Examination.

from Tianjin Huanhu Hospital; QL_W from Qilu Hospital; and XW_H and XW_Z from Xuanwu Hospital of Capital Medical University). Table 2 lists the demographic and clinical information for all subjects in both cohorts (details for each site are listed in the Supplemental material online). Details regarding the subjects' information are given in the Supplementary text (online).

2.2. Image acquisition and data preprocessing

All subjects were scanned by functional MRI, diffusion MRI, and structural MRI; the data were collected on 3.0 T MRI scanners with standard head coil. For all the sites, to ensure high-quality data acquisition, the scanning protocols were set up by experienced experts to achieve harmonized imaging quality at the different sites with different types of MRI scanners. The parameters of the fMRI scans from the six centers are provided in the Supplementary material (Table S1 online). To minimize the variation in multicenter data, we included the following quality controls: (1) exclusion of subjects with poor fMRI data quality, subjects without complete demographic information and subjects without Mini-Mental State Examination (MMSE) scores; (2) removal of subjects with large head motion in any direction corresponding to >3 mm or any rotation >3°; and (3) matching the age and gender of the subjects at each center.

All rs-fMRI data were preprocessed in a standard pipeline using the Brainnetome Toolkit (BRANT, http://brant.brainnetome.org) [50], utilized by several previous studies [21,51,52] (here we still provide a brief introduction to maintain the scientific integrity), as follows: (1) deletion of the first 10 time points and slice timing; (2) realignment to the first volume; (3) spatial normalization to the Montreal Neurological Institute (MNI) space and resampling to 2 mm × 2 mm × 2 mm; (4) regression of nuisance signals, including linear trend, six motion parameters and their first-order differences, and the mean signals of the white matter and cerebrospinal fluid; (5) bandpass temporal filtering (0.01–0.08 Hz) to reduce high-frequency noise; and (6) smoothing with a 6 mm full-width half-maximum (FWHM) kernel. It has been shown that even small head motion during fMRI scanning has an impact on some indices of rs-fMRI [53–55]. We evaluated group differences in head motion between the two groups for mean translation and mean rotation, and the results showed no significant differences in the head motion of each MRI scanner (all $P > 0.1$).

2.3. Brain activity measurement

For a voxel x, AM was defined as the mean absolute value of the deviation of the BOLD fMRI signal from the mean value of its whole time series [21]:

$$AM = \frac{1}{N}\sum_{j}^{N} |x(j) - \bar{X}|, \quad (1)$$

where $x(j)$ is the value of the voxel x at time j, and $\bar{X}$ is the mean of the time series of the voxel. AM is highly correlated with the previously widely used measure ALFF [21]. To reduce the effect of the individual variance, the normalized amplitude of the activity map was computed by dividing it by the mean AM of the whole brain for each subject [21].

2.4. Mega-analysis

For each dataset, two-sample t-tests were performed between AD and NC subjects after controlling for age and gender effects. In this way, the activity of each voxel had six P values for six datasets. Then, we used the Stouffer Z-score method, which has optimal power for combining probabilities in meta-analysis [56–58]. Specifically, for each voxel, the P value of each dataset was transformed into the corresponding Z statistic through the inverse standard normal distribution [58,59]. Then, the combined Z statistic was computed by the following formula [60]:

$$Z = \frac{\sum_{i=1}^{k} z_i}{\sqrt{k}}, \quad (2)$$

where k is the number of datasets (here, $k = 6$). Under the null hypothesis, the Z statistic follows the standard normal distribution. Therefore, by converting the Z-scores to the corresponding P values, we identified significantly changed amplitudes of spontaneous activity in AD patients at $P < 0.05$ (Bonferroni corrected, cluster size larger than 50 voxels). This step was performed with the "IBMA" function under "STAT" within the BRANT toolkit (BRANT, http://

brant.brainnetome.org). The heterogeneity of the altered brain activity within the identified brain regions was additionally assessed using a random-effects model after controlling for age, gender and site effects [36,61]. This step was performed with the package "metafor" (http://www.metafor-project.org/).

2.5. Multivariate classification

The above analyses provide maps of structural brain differences between AD and NC subjects. To assess the multivariate performances of these activity features, we used support vector machine (SVM) (http://www.csie.ntu.edu.tw/~cjlin/libsvm/) techniques to create a multivariate classifier that provides individual level prediction of group status. SVM is a widely used classifier method that has been extensively validated for many similar high-dimensional pattern recognition issues. The input features were the resliced raw amplitude maps (resolution 6 mm × 6 mm × 6 mm) of brain activity of each voxel of each subject.

To maximize the generalizability of the present study, we applied the SVM classification with a radial basis function (RBF) kernel using default parameters ($C = 4$, $g = 2^{-5}$), with the top 2000 voxels using *t*-test feature selection [62,63]. We performed training and testing steps using the leave-one-site-out cross-validation method to improve the predictive power [64–67]. This procedure guarantees an evaluation of the generalizability of the classifier based on independent new data from entirely different sites. For all analyses, individual subject classification performances were evaluated by accuracy (ACC), sensitivity (SEN) and specificity (SPE) values based on leave-one-site-out cross-validation. The diagnostic capabilities of the features used were also evaluated with receiver operating characteristic (ROC) curves and summarized using the area under the ROC curve (AUC) [67].

2.6. Correlation analysis

To further evaluate whether the activity in the identified brain areas changed with disease progression, we performed a correlation analysis of the mean amplitude of the identified brain areas and the degree of cognitive impairment (MMSE) after regressing out age, gender and site effects.

To evaluate the clinical relevance of the activity-based classification results, we also assessed the correlations between MMSE scores and the classifier output of each individual subject [67]. For this analysis, individual classifier output was defined by the distance to the hyperplane, and the scores were normalized by Z-scores within each site.

2.7. Comparison of altered activity fingerprinting to the changes in metabolism and amyloid in AD patients

To compare the anatomical MNI locations of the identified map with the distribution of Aβ accumulation and hypometabolism, we introduced the results from Prof. G. Chetelat's laboratory [68]. Specifically, Z-score maps of metabolism (FGD-PET) and amyloid deposition (AV45-PET) were computed and averaged for 26 Aβ-positive AD patients. The Z-score maps were computed using a group of 52 cognitively normal controls as a reference. All controls had a negative AV45-PET scan and were matched for age, sex and education with the patient group. Before computing Z-score maps, images were preprocessed using a standard pipeline implemented in SPM12. All images were in the MNI space, and differential Gaussian kernel smoothing was applied to each neuroimaging map to obtain equivalent data with an effective FWHM smoothing kernel = 10 mm [69]. For the regions identified as having altered brain activity, we performed a correlation analysis between the Z-score of our mega-map (increasing and decreasing maps were plotted separately) and the changes in metabolism (FGD-PET) and amyloid (AV45-PET) maps. Note that decreased metabolism in patients corresponded to negative Z-scores, while increased amyloid pathology corresponded to positive Z-scores.

3. Results

3.1. Demographic and clinical characteristics

There were no significant differences in the age ($P = 0.07$ to 0.75) or sex (0.13 to 0.75) of the AD, aMCI and NC subjects at each site. Subjects of the aMCI and AD groups exhibited significantly lower scores on the MMSE than those of the NC group ($P < 0.001$) (Table 2).

3.2. Alerted brain activity map in AD

We found significant differences between AD patients and NCs at each single center (Fig. S1 online). Compared with those of NCs, AD patients showed significantly lower spontaneous brain activity (normalized amplitude) in the default mode network (including the PCC/PCu, bilateral angular gyrus, superior frontal gyrus and left orbitofrontal region) (Fig. 2, Table S2 online). The AD patients showed increased strength of brain activity in the bilateral hippocampus/parahippocampus, caudate nucleus, orbital part of the middle frontal gyrus (MFG), thalamus, and left fusiform (Fig. 2). Further investigation showed that aMCI subjects showed an AD-like altered pattern (Fig. 2).

Moreover, the altered patterns of spontaneous brain activity were very consistent across data sets from the 6 different sites despite differences in the scanners and studied populations (Fig. 3). The mean strength of the decreasing brain activity maps was highly consistent between AD patients and NCs; for regions of increased activity, only the caudate and parahippocampus at one of the six centers showed a very slight discordance (Fig. 3).

3.3. Associations between brain activity and clinical cognitive scores

To determine whether disease severity was related to altered spontaneous activities, we performed a correlation analysis between the strength of brain activity within the identified brain regions and cognitive abilities (MMSE scores) in AD and aMCI subjects after controlling for age, gender and site effects. Significant positive correlations between the mean brain activity strength and the MMSE scores were observed for the regions showing decreased spontaneous brain activity in AD (range of the correlation $r = 0.1571$–0.2942, all $P < 0.001$) (Fig. 4). Furthermore, the mean brain activity strength was negatively correlated with MMSE scores in the regions with increased activity (ranged from $r = -0.2969$ to -0.1345, $P < 0.0001$–0.0034) (Fig. 4).

3.4. Multivariate classification is accurate using leave-one-site-out cross-validation

The classification had a mean ACC of 78.49% ± 6.82%, a mean SPE of 75.52% ± 15.55%, and a mean SEN of 82.72% ± 10.98% with leave-one-site-out cross-validation (Fig. 5a). An AUC value of 0.824 was achieved (Fig. 5b, red line). More importantly, we found a significant correlation ($r = 0.547$, $P = 8.67 \times 10^{-38}$) between the individual distance to the hyperplane and MMSE scores in AD and aMCI individuals as well as a significant correlation ($r = 0.280$, $P = 6.61 \times 10^{-6}$) in the AD group (Fig. 5c). The areas with the best discriminative performance for distinguishing AD patients from NCs were highly overlapped with the altered patterns we found across sites (Fig. 5d).

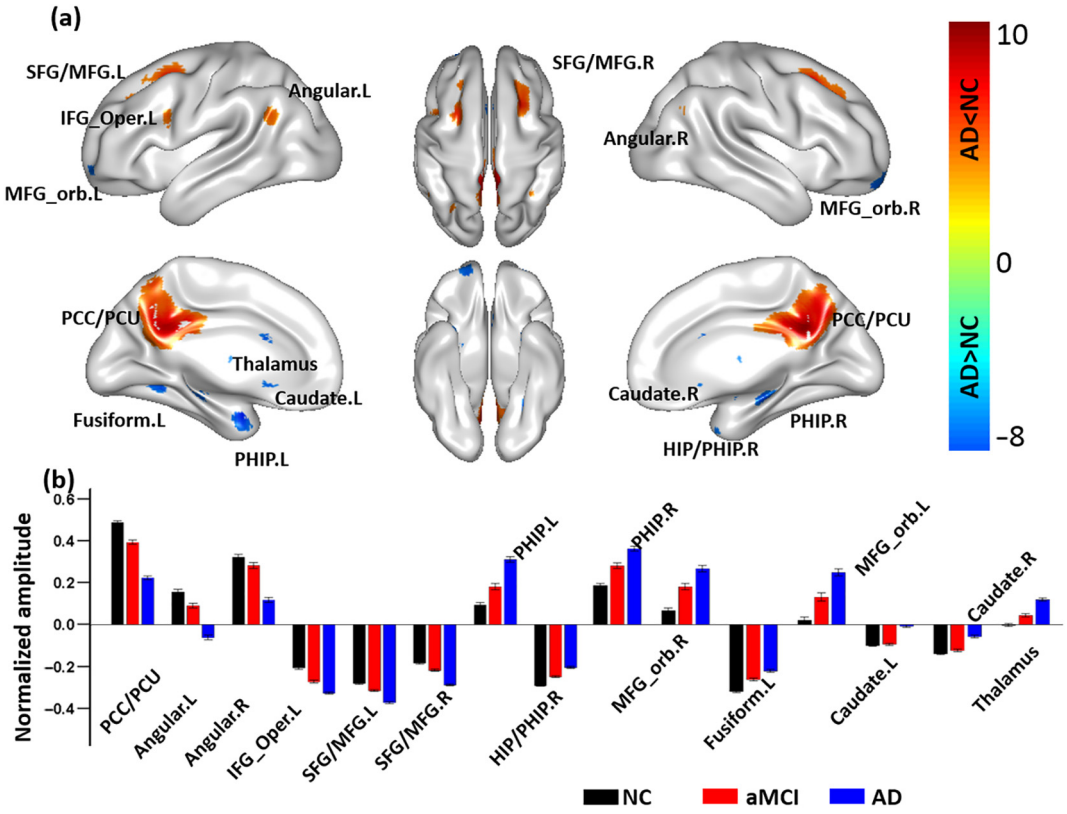

Fig. 2. Regions that showed significant alterations in brain spontaneous activity in AD patients compared with those in normal controls. (a) Key regional activity differences between patients (AD) and controls (NC) ($P < 0.05$, Bonferroni corrected). (b) Mean amplitude index among NC (black), MCI (red) and AD (blue) subjects in the identified regions ($P < 0.05$, Bonferroni corrected) after regressing out age, gender and site effects. Abbreviations: PCC = posterior cingulate cortex; PCu = precuneus; IFG_Oper = inferior frontal gyrus and orbitofrontal parts; SFG = superior frontal gyrus; MFG = medial frontal gyrus; HIP = hippocampus; PHIP = parahippocampus; L = left; R = right.

3.5. Amyloid-β accumulation and hypometabolism deposition in AD occurs preferentially in the cortical regions where altered activity is identified

Activity properties in certain cortical regions may reflect metabolic alterations or Aβ accumulation. Thus, we assessed the topographic similarity between the level of altered activity amplitude and the typical pattern of hypometabolism and Aβ deposition in AD. (1) Correlation with amyloid PET: The Z-scores in the regions with decreased AM patterns showed a significant positive correlation ($r = 0.5995$, $P < 0.0001$) with the Z-scores of Aβ accumulation in the same regions, i.e., greater altered (decreased) AM was found in regions with more Aβ accumulation in AD (Fig. 6a). The Z-scores in the regions with increased AM patterns showed a significant negative correlation ($r = 0.2029$, $P < 0.0001$) with the Z-scores of Aβ accumulation, i.e., regions with greater altered (increased) AM had lower Aβ accumulation in AD (Fig. 6b). (2) Correlation with FDG-PET: The Z-scores in the regions with decreased AM patterns showed a significant positive correlation ($r = 0.4406$, $P < 0.0001$) with hypometabolism, i.e., regions with greater altered (decreased) AM had greater hypometabolism in AD (Fig. 6c). The regions with increased AM patterns did not show a significant correlation ($r = 0.0232$, $P = 0.3679$) with metabolism (Fig. 6d).

3.6. Data availability

The patients' normalized brain activity maps and the open Brainnetome fMRI toolkit are available online at https://github.com/yongliulab. The data used are available from the author (Y. L) upon reasonable request.

4. Discussion

In the present study, we conducted a novel large-scale analysis of rs-fMRI data pooled from 6 sites to demonstrate robust and reproducible abnormal brain activity in AD dementia patients compared with that in NCs across sites. The aMCI patients showed alterations similar to those of AD patients and fell into an intermediate stage between the NC and AD subjects. Furthermore, the abnormality in brain areas was significantly correlated with objective cognitive performance in the AD/aMCI groups. Notably, a simple SVM classification analysis highlighted the reproducibility of the altered brain activity patterns and the feasibility of using these patterns as a hallmark for AD diagnosis. Finally, correlation analysis between the mega-altered maps of brain spontaneous activity and the alterations revealed by PET data highly emphasize the pathophysiological significance of altered brain activity in the corresponding brain areas of AD patients. This profile indicates the potential of using spontaneous activity patterns in the resting state as biomarkers or predictors of MCI/AD.

4.1. Robust and replicated abnormal activity in AD

Previous studies provided compelling evidence that anatomical and functional alterations in brain regions of the default mode network (especially in the PCu, lateral temporo-parietal cortex, and medial frontal cortex) are particularly important imaging markers of disease severity and cognitive decline [21,70–72]. The regions in the default mode network are clarified relative to episodic memory and the processing of cognitive tasks [73,74]. Regional brain hypometabolism of the PCC/PCu is related to the global amyloid burden,

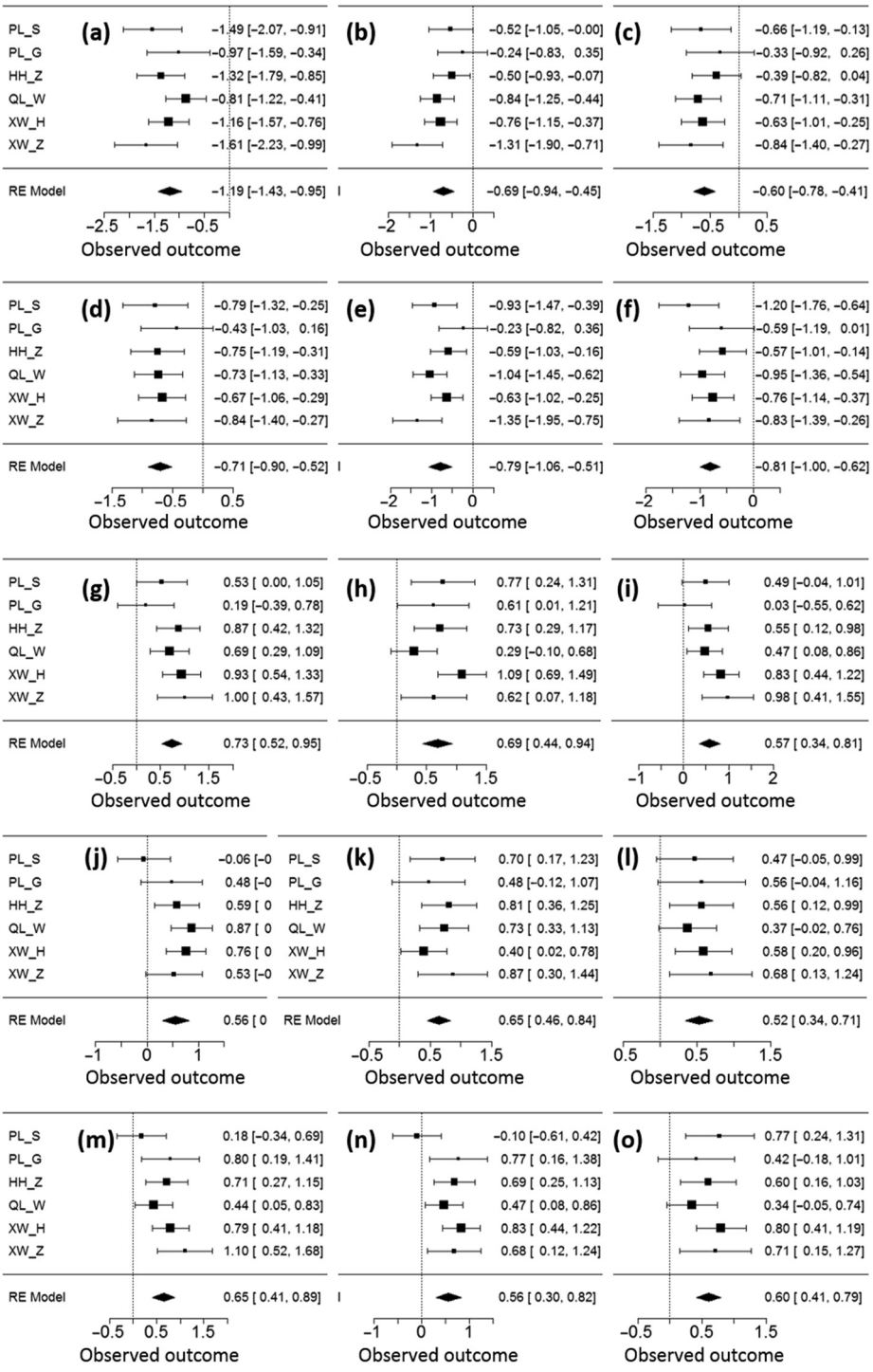

Fig. 3. Forest plots showing a meta-analysis of the association of the significantly altered AM of spontaneous brain activity with AD. The results showed that the altered patterns of AM were consistent across the data sets from the six different imaging centers. (a) Posterior cingulate cortex/precuneus; (b) left Angular; (c) right Angular; (d) left inferior frontal gyrus and orbitofrontal parts; (e) left superior frontal gyrus and medial frontal gyrus; (f) right superior frontal gyrus and medial frontal gyrus; (g) left parahippocampus; (h) right parahippocampus/ahippocampus; (i) right parahippocampus; (j) right medial frontal gyrus orbitofrontal parts; (k) left fusiform gyrus; (l) right medial frontal gyrus orbitofrontal parts; (m) left caudate nucleus; (n) right caudate nucleus; (o) thalamus.

which is an important hallmark of AD [75]. Previous studies also demonstrated that decreased metabolism in the PCC is present in the very early stage of AD [76–78]. On the other hand, decreased brain activity in the parahippocampal gyrus and the fusiform gyrus may also cause memory deficits, and lower brain activity in the angular gyrus may contribute to the poor verbal working memory ability of AD patients [42]. In the distributed pattern of pathologic alterations in AD, the default mode network was demonstrated to be vulnerable according to multimodal imaging assessments and showed spatially specific amyloid deposition, atrophy and hypometabolism [72,79,80]. Reduced gray matter volume [81,82] and consistent connectivity alterations in inter- and intranetworks of the default mode network [83] have been reported in MCI/AD patients compared with those in NCs, and these findings are

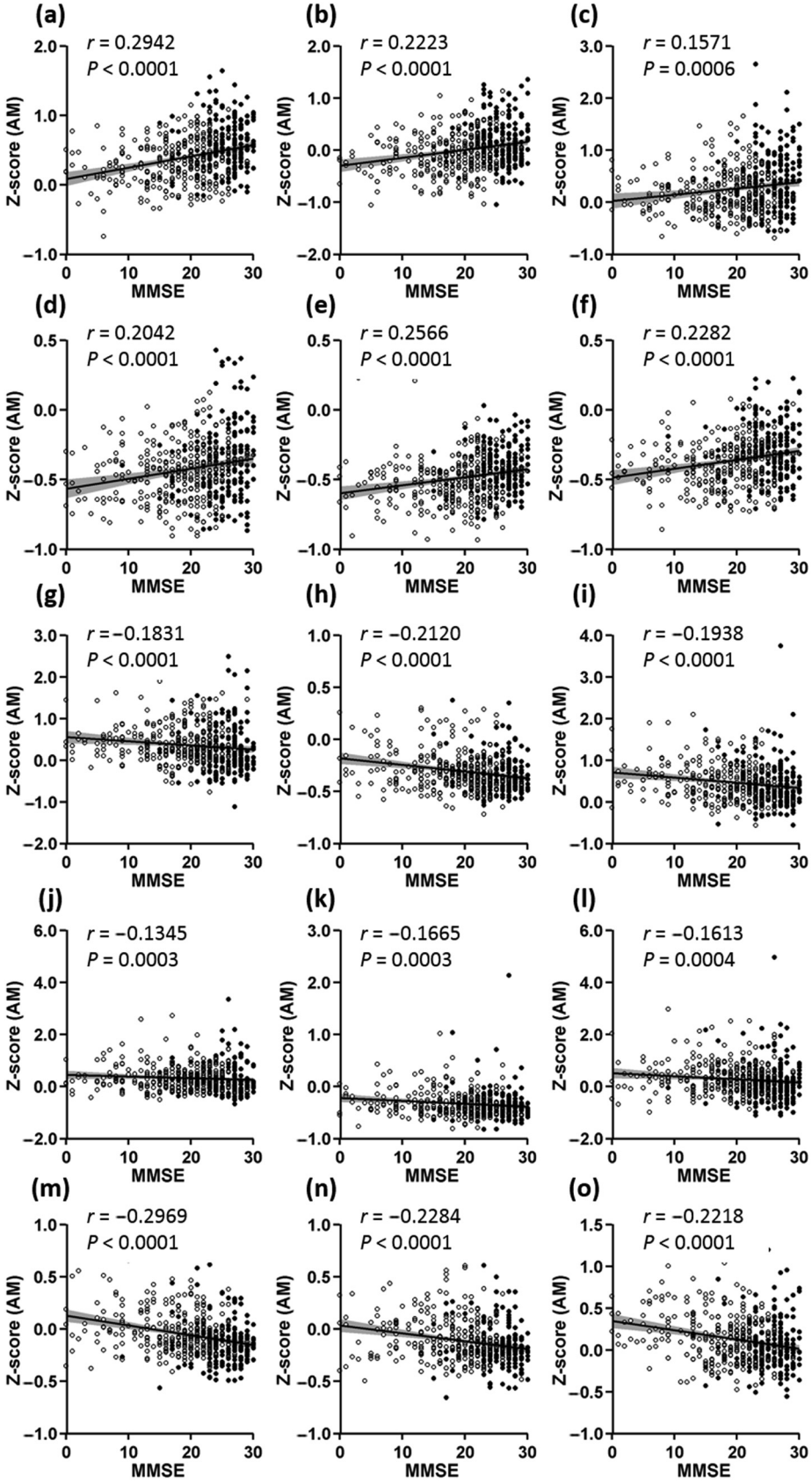

Fig. 4. Scatter plot showing the relationship between MMSE scores and amplitudes of the identified brain regions in AD and aMCI subjects. Black dot represent AD subjects, and black circle represent aMCI subjects. (a) Posterior cingulate cortex/precuneus; (b) left Angular; (c) right Angular; (d) left inferior frontal gyrus and orbitofrontal parts; (e) left superior frontal gyrus and medial frontal gyrus; (f) right superior frontal gyrus and medial frontal gyrus; (g) left parahippocampus; (h) right parahippocampus/ahippocampus; (i) right parahippocampus; (j) right medial frontal gyrus orbitofrontal parts; (k) left fusiform gyrus; (l) right medial frontal gyrus orbitofrontal parts; (m) left caudate nucleus; (n) right caudate nucleus; (o) thalamus.

(a)

	ACC	SPE	SEN
PL_S	75.29	58.54	90.91
PL_G	77.78	80.95	75.00
HH_Z	80.33	100.00	67.57
QL_W	74.77	69.05	78.46
XW_H	71.68	60.61	87.23
XW_Z	91.07	80.95	97.14
Mean	78.49±6.82	75.52±15.55	82.72±10.98

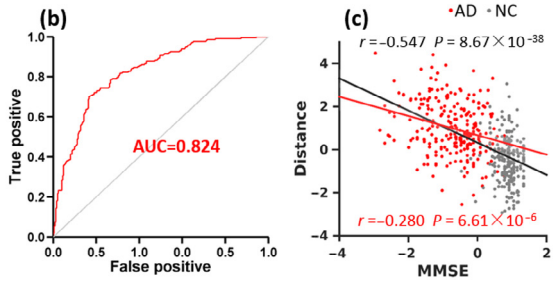

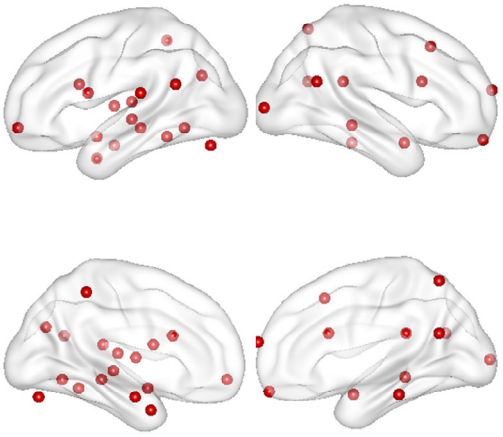

Fig. 5. Classification results of leave-one-site-out cross-validation with brain activity as a feature. (a) The classification results (ACC, SPE and SEN) with one site as the validation cohort and the remaining sites as the discovery cohort. (b) ROC curve for classification of AD patients versus control subjects with brain activity. (c) Correlation between classifier output (distances of the test samples from the discrimination hyperplane) and MMSE scores. The correlation of the classifier score with MMSE score was equal to $r = -0.547$ ($P < 0.001$) in the AD and NC groups and $r = -0.280$ ($P < 0.001$) in the AD group. (d) The regions that yield the best discrimination performance for distinguishing AD patients from normal controls (here, only seed regions of the brain regions identified in 4 of the 6 sites cross validations are given).

supported by the potent abnormal reduction in brain activity observed in the present study. Furthermore, significant correlations between the resting-state activity of the default mode network and cognitive ability (measured with MMSE scores) in MCI and AD suggest that the changes in brain activity in this network are associated with altered cognitive performance. Positive correlations were observed between the altered activity Z-maps and the independent Z-maps from PET images, indicating that the altered activity map partially reflects the pathophysiological abnormalities in AD.

Increased brain activity was observed mainly in the bilateral hippocampus/parahippocampus, thalamus, caudate nucleus, orbital part of the medial prefrontal cortex (MPFC) and left fusiform. The hippocampus is widely known to be critical for memory, cognition and learning and is primarily and generally affected in AD [84,85]. Within the hippocampus, progressively increased hyperactivity has been demonstrated in patients with aMCI and AD dementia [19,22,24,28,86], which might be due to disconnections from the default mode network [87], eventually resulting in abnormal brain activity. Conversely, the fusiform gyrus has been reported to be involved in a mechanism compensating for the decreased brain activity in other brain regions and to maintain cognitive performance in AD [18,19,28].

4.2. Relationship between brain activity and cognitive ability

In line with several previous studies, the present results demonstrated that all the identified regions showed significant correlations between the amplitude of brain activity and cognitive ability scores, which may provide important clues regarding the underlying pathological profiles of disease-associated variability in AD/aMCI [21]. We also noted that the variance was still relatively high in some regions, which might have been due to the different subtypes of patient groups or variance at different sites. More importantly, a very strong correlation was found between the classification output and cognitive ability scores, which indicated that the brain activity pattern is a potential imaging marker for AD/aMCI and confirmed that the identified regions substantially contribute to classification.

Hypometabolism is reportedly localized to mainly the PCC and the temporo-parietal lobe in AD patients [68,88], and Aβ accumulation has also been found in the PCC [68]. Previous studies documented a significant correlation between spontaneous brain activity and glucose metabolism in these regions [89,90], and these correlations were significantly lower in aMCI/AD patients [90]. To further validate our findings, we evaluated the correlation between the presently identified Z-scores and the altered Z-maps of amyloid PET and FDG-PET. The decreased Z-scores that we identified were found to have a highly significant, positive correlation with amyloid PET and FDG-PET, which means that the severity of impaired brain activity is in some way linked to abnormal glucose utilization in brain regions that are impacted by the underlying pathological alteration [90].

4.3. Consensus imaging marker for classifying AD

Biomarkers are objective biological measures that can predict clinical outcomes for the optimization of individualized care. Neuroimaging techniques, such as structural and functional MRI, provide an opportunity to advance previous group comparison analyses into an era of subjective descriptive classification [91,92]. In particular, leave-one-out (or *n*-fold) cross-validation pipelines, which remove single samples (or random subsamples), have become very popular in the past decades for analyzing small sample sizes in single-center studies. However, these types of models do not have high predication performance when applied to new datasets, which might be the reason that neuroimaging, especially brain imaging, has yet to substantially impact public health despite its great promise [93]. Instead of leaving out random subsamples from testing, the leave-one-site-out cross-validation method leads to the identification of brain activity biomarkers of AD that are replicable and robust while considering uncontrolled intersite variability [65,94]. The current results demonstrated the practicability of using intersite heterogeneous datasets to identify brain imaging biomarkers that are robust among different sites. Indeed, the mean ACC of 78.5% is comparable to the ACC values reported in previous fMRI-based studies [16,28]. We admit that better classification results can potentially be achieved by improving feature selection, tuning the model parameters, or other potential improvement methods, such as deep learning. However, these approaches might lead to the risk of overfitting or reduce the

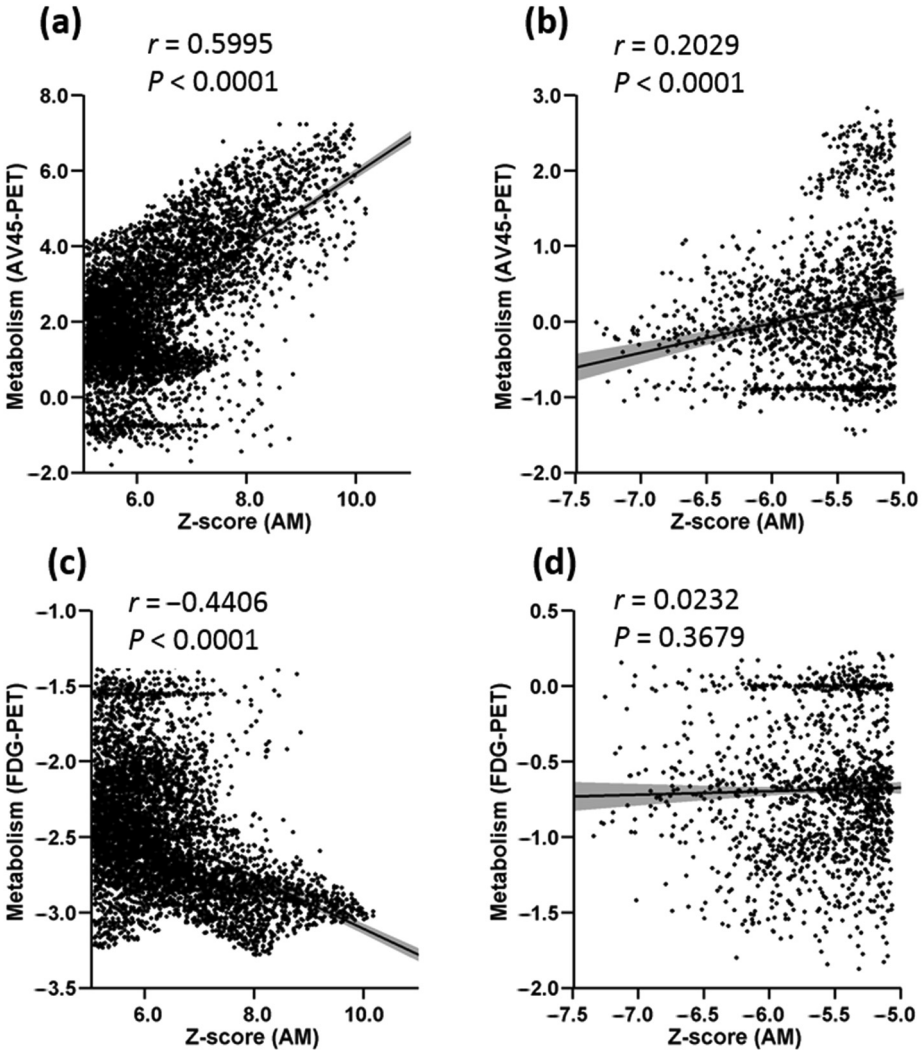

Fig. 6. Relationship between altered metabolism results and the current findings. (a) The Z-scores in the regions with decreased AM patterns showed a significant positive correlation ($r = 0.5995$, $P < 0.0001$) with the Z-scores of Aβ accumulation in the same regions. (b) The Z-scores in the regions with increased AM patterns showed a significant negative correlation ($r = 0.2029$, $P < 0.0001$) with the Z-scores of Aβ accumulation. (c) The Z-scores in the regions with decreased AM patterns showed a significant positive correlation ($r = 0.4406$, $P < 0.0001$) with hypometabolism. (d) The Z-scores in the regions with increased AM patterns did not show a significant correlation ($r = 0.0232$, $P = 0.3679$) with metabolism.

generalizability of the results to data obtained from new, independent scanners, as suggested by a previous multisite imaging study [67]. Hence, an important finding of the present study was that the classifier could retain relatively high prediction accuracy when trained and tested on independent datasets. More importantly, the consensus features largely overlap with the identified brain regions, further emphasizing the potential for brain activity patterns to be a robust and reproducible imaging signature of AD.

4.4. Caveats, limitations, and future directions

As suggested by a previous report [95], the present study comprised an imaging-based meta-analysis using data from 6 centers rather than reporting the results of previous studies via a coordinate-based meta-analysis. Image-based meta-analysis (IBMA) might provide powerful and reproducible results of meta-analyses based on published work and might retain less information from each individual study [95]. For example, the altered brain activity information in the parahippocampus may be lost if only postprocessed data, such as the "PL_G" data shown in Fig. 3i, are considered. We must caution that researchers should explore better data sharing strategies and employ careful quality control measures for acquiring data.

Certain limitations should be noted. First, although the present study benefited from a large sample size consisting of 6 sites, an unavoidable limitation is that the inclusion and exclusion criteria of each site may have slightly differed; despite trying our best to include only data that used the same diagnostic criteria, subject heterogeneity might have partially influenced the statistical results. Second, brain abnormalities in AD patients cannot be one hundred percent confirmed without PET data [11]. This potential risk is largely reduced for patients who are diagnosed by experienced neurologists, and most of the included data have already been used in published studies [21,96–101]. Further correlation analyses between the altered activity pattern and the altered FDG-PET and amyloid PET maps confirmed the physiological significance of the identified impaired brain activity. Meanwhile, we should note that the correct ratio in the present study is still not high enough for clinical application and beyond the AM index to describe local brain activities; thus, other imaging indices (such as gray matter volume, cortical thickness) need to be employed for a more accurate classification of AD patients. In fact, we added

the gray matter volumes of the identified brain regions as additional features, and the AUC improved from 0.824 to 0.969 (see the Supplemental materials for details, Fig. S2 online). Hence, we concluded that brain activity is an additional measure for distinguishing AD patients from NCs. Next, we plan to carefully study other measures, such as the network architecture of the whole brain [102], functional connectivity density, gray matter volume [103], cortical thickness and texture of important brain regions [63], in AD to determine more powerful and robust features based on these datasets. All the results, including the pipeline codes, will be shared online and open for researchers to build better pattern recognition algorithms for potential clinical applications.

We should also note that the image acquisition scanning protocols differed across the studied sites; therefore, the variations in scanning parameters (for example, time of echo, voxel size, scan time duration) could have limited the analysis of the fMRI data among the different sites. It would be better to minimize the inconsistencies in the image parameters for group analyses in future multisite studies. Finally, although we found a consistent pattern across multiple sites by mega-analysis of the statistical map of each site, it should be noted that variations in the distribution of participants or observations between datasets may obfuscate real effects when datasets are combined [104]. All included samples were processed using identical analysis pipelines and with stringent quality control procedures, thus minimizing the heterogeneity of the different preprocessing methods. On the other hand, site variance should be taken into consideration in future application studies. A previous study conducted using data acquired from 5 German sites was performed to assess the site effect and how to reduce the limitation regarding the use of multicenter acquired rs-fMRI data. The authors suggested that the decreased group effect was mainly due to multiscanner variability, and visual inspection of the data or quality could reduce the majority of the variability [35]. Hence, future efforts should attempt to validate this pattern at independent sites with large longitudinal clinical samples.

5. Conclusion

The novelty of the present study is that we identified the brain regions showing the most severe and robust impairment in spontaneous activity in AD patients using six independent datasets. The image-based mega-analysis, correlation and predication analysis based on intersite data, with additional correlation analysis between mega z-maps and independent Z-maps from PET data, provide more comprehensive and conclusive findings of abnormal brain activity in AD. Taken together, these results highlight the reproducibility of spontaneous brain activity patterns and provide new insights into evaluating brain pathology in AD and, therefore, its translational potential.

Conflict of interest

The authors declare that they have no conflict of interest.

Acknowledgments

This work was partially supported by the National Key Research and Development Program of China (2016YFC1305904, 2016YFC1306300), the National Natural Science Foundation of China (81871438, 61633018, 81571062, 81471120, 61431012, 81430037), the Strategic Priority Research Program (B) of Chinese Academy of Sciences (XDB32020200), and the Beijing Municipal Commission of Health and Family Planning (PXM2019_026283_000002).

Author contributions

Jiachen Li, Dan Jin and Yong Liu analyzed the data and performed the measurements; Ying Han, Tong Han, Jie Lu, Chengyuan Song, Pan Wang, Dawei Wang, Qing Wang, Hongwei Yang, Hongxiang Yao, Chunshui Yu, Bo Zhou, Xinqing Zhang, Yuying Zhou, and Xi Zhang collected the data; Alexandre Bejanin and Gael Chetelat provided the PET results. Jiachen Li and Yong Liu were majorly responsible for preparing the manuscript; and Dan Jin, Ang Li, Bing Liu, Kaibin Xu, Chunshui Yu and Tianzi Jiang revised the manuscript. Yong Liu and Ying Han supervised the project.

Appendix A. Supplementary data

Supplementary data to this article can be found online at https://doi.org/10.1016/j.scib.2019.04.034.

References

[1] Albert MS, DeKosky ST, Dickson D, et al. The diagnosis of mild cognitive impairment due to Alzheimer's disease: recommendations from the National Institute on Aging-Alzheimer's Association workgroups on diagnostic guidelines for Alzheimer's disease. Alzheimers Dement 2011;7:270–9.
[2] Albert M, Zhu Y, Moghekar A, et al. Predicting progression from normal cognition to mild cognitive impairment for individuals at 5 years. Brain 2018;141:877–87.
[3] McKhann GM, Knopman DS, Chertkow H, et al. The diagnosis of dementia due to Alzheimer's disease: recommendations from the National Institute on Aging-Alzheimer's Association workgroups on diagnostic guidelines for Alzheimer's disease. Alzheimers Dement 2011;7:263–9.
[4] Chan KY, Wang W, Wu JJ, et al. Epidemiology of Alzheimer's disease and other forms of dementia in China, 1990–2010: a systematic review and analysis. Lancet 2013;381:2016–23.
[5] Prince M, Comas-Herrera A, Knapp M, et al. World Alzheimer report 2016: improving healthcare for people living with dementia. Alzheimer's Disease International 2016.
[6] Ikonomovic MD, Klunk WE, Abrahamson EE, et al. Post-mortem correlates of in vivo PiB-PET amyloid imaging in a typical case of Alzheimer's disease. Brain 2008;131:1630–45.
[7] Dubois B, Feldman HH, Jacova C, et al. Advancing research diagnostic criteria for Alzheimer's disease: the IWG-2 criteria. Lancet Neurol 2014;13:614–29.
[8] Wang L, Benzinger TL, Su Y, et al. Evaluation of tau imaging in staging Alzheimer disease and revealing interactions between beta-amyloid and tauopathy. JAMA Neurol 2016;73:1070–7.
[9] Gordon BA, Blazey T, Su Y, et al. Longitudinal beta-amyloid deposition and hippocampal volume in preclinical Alzheimer disease and suspected non-Alzheimer disease pathophysiology. JAMA Neurol 2016;73:1192–200.
[10] Sperling RA, Aisen PS, Beckett LA, et al. Toward defining the preclinical stages of Alzheimer's disease: recommendations from the National Institute on Aging-Alzheimer's Association workgroups on diagnostic guidelines for Alzheimer's disease. Alzheimers Dement 2011;7:280–92.
[11] Jack Jr CR, Bennett DA, Blennow K, et al. NIA-AA research framework: toward a biological definition of Alzheimer's disease. Alzheimers Dement 2018;14:535–62.
[12] Barkhof F, Haller S, Rombouts SA. Resting-state functional MR imaging: a new window to the brain. Radiology 2014;272:29–49.
[13] Brier MR, Gordon B, Friedrichsen K, et al. Tau and Aβ imaging, CSF measures, and cognition in Alzheimer's disease. Sci Transl Med 2016;8:338ra66.
[14] Zang YF, He Y, Zhu CZ, et al. Altered baseline brain activity in children with ADHD revealed by resting-state functional MRI. Brain Dev 2007;29:83–91.
[15] Bijsterbosch J, Harrison S, Duff E, et al. Investigations into within- and between-subject resting-state amplitude variations. Neuroimage. 2017;159:57–69.
[16] de Vos F, Koini M, Schouten TM, et al. A comprehensive analysis of resting state fMRI measures to classify individual patients with Alzheimer's disease. Neuroimage 2017;167:62–72.
[17] Zhou Y, Yu F, Duong TQ, et al. White matter lesion load is associated with resting state functional MRI activity and amyloid PET but not FDG in mild cognitive impairment and early Alzheimer's disease patients. J Magn Reson Imaging 2015;41:102–9.
[18] He Y, Wang L, Zang Y, et al. Regional coherence changes in the early stages of Alzheimer's disease: a combined structural and resting-state functional MRI study. Neuroimage 2007;35:488–500.
[19] Wang Z, Yan C, Zhao C, et al. Spatial patterns of intrinsic brain activity in mild cognitive impairment and Alzheimer's disease: a resting-state functional MRI study. Hum Brain Mapp 2011;32:1720–40.
[20] Song J, Qin W, Liu Y, et al. Aberrant functional organization within and between resting-state networks in AD. PLoS One 2013;8:e63727.

[21] Liu Y, Yu C, Zhang X, et al. Impaired long distance functional connectivity and weighted network architecture in Alzheimer's disease. Cereb Cortex 2014;24:1422–35.
[22] Liu X, Wang S, Zhang X, et al. Abnormal amplitude of low-frequency fluctuations of intrinsic brain activity in Alzheimer's disease. J Alzheimers Dis 2014;40:387–97.
[23] Weiler M, Teixeira CV, Nogueira MH, et al. Differences and the relationship in default mode network intrinsic activity and functional connectivity in mild Alzheimer's disease and amnestic mild cognitive impairment. Brain Connect 2014;4:567–74.
[24] Liang P, Xiang J, Liang H, et al. Altered amplitude of low-frequency fluctuations in early and late mild cognitive impairment and Alzheimer's disease. Curr Alzheimer Res 2014;11:389–98.
[25] Cha J, Hwang JM, Jo HJ, et al. Assessment of functional characteristics of amnestic mild cognitive impairment and Alzheimer's disease using various methods of resting-state FMRI analysis. Biomed Res Int 2015;2015:907464.
[26] Wen X, Wu X, Li R, et al. Alzheimer's disease-related changes in regional spontaneous brain activity levels and inter-region interactions in the default mode network. Brain Res 2013;1509:58–65.
[27] Mascali D, DiNuzzo M, Gili T, et al. Intrinsic patterns of coupling between correlation and amplitude of low-frequency fMRI fluctuations are disrupted in degenerative dementia mainly due to functional disconnection. PLoS One 2015;10:e0120988.
[28] Dai Z, Yan C, Wang Z, et al. Discriminative analysis of early Alzheimer's disease using multi-modal imaging and multi-level characterization with multi-classifier (M3). Neuroimage 2012;59:2187–95.
[29] Wang X, Wang J, He Y, et al. Apolipoprotein E epsilon4 modulates cognitive profiles, hippocampal volume, and resting-state functional connectivity in Alzheimer's disease. J Alzheimers Dis 2015;45:781–95.
[30] Poldrack RA, Poline JB. The publication and reproducibility challenges of shared data. Trends Cogn Sci 2015;19:59–61.
[31] Biswal BB, Mennes M, Zuo XN, et al. Toward discovery science of human brain function. Proc Natl Acad Sci USA 2010;107:4734–9.
[32] Wang X, Jiao Y, Tang T, et al. Investigating univariate temporal patterns for intrinsic connectivity networks based on complexity and low-frequency oscillation: a test-retest reliability study. Neuroscience 2013;254:404–26.
[33] Button KS, Ioannidis JP, Mokrysz C, et al. Power failure: why small sample size undermines the reliability of neuroscience. Nat Rev Neurosci 2013;14:365–76.
[34] Dillen KNH, Jacobs HIL, Kukolja J, et al. Aberrant functional connectivity differentiates retrosplenial cortex from posterior cingulate cortex in prodromal Alzheimer's disease. Neurobiol Aging 2016;44:114–26.
[35] Teipel SJ, Wohlert A, Metzger C, et al. Multicenter stability of resting state fMRI in the detection of Alzheimer's disease and amnestic MCI. Neuroimage Clin 2017;14:183–94.
[36] Borenstein M, Hedges LV, Higgins JPT, et al. Introduction to meta-analysis. West Sussex: John Wiley & Sons, Ltd; 2009.
[37] Nellessen N, Rottschy C, Eickhoff SB, et al. Specific and disease stage-dependent episodic memory-related brain activation patterns in Alzheimer's disease: a coordinate-based meta-analysis. Brain Struct Funct 2015;220:1555–71.
[38] Jacobs HI, Gronenschild EH, Evers EA, et al. Visuospatial processing in early Alzheimer's disease: a multimodal neuroimaging study. Cortex 2015;64:394–406.
[39] Browndyke JN, Giovanello K, Petrella J, et al. Phenotypic regional functional imaging patterns during memory encoding in mild cognitive impairment and Alzheimer's disease. Alzheimers Dement 2013;9:284–94.
[40] Li HJ, Hou XH, Liu HH, et al. Toward systems neuroscience in mild cognitive impairment and Alzheimer's disease: a meta-analysis of 75 fMRI studies. Hum Brain Mapp 2015;36:1217–32.
[41] Pan P, Zhu L, Yu T, et al. Aberrant spontaneous low-frequency brain activity in amnestic mild cognitive impairment: a meta-analysis of resting-state fMRI studies. Ageing Res Rev 2017;35:12–21.
[42] Lau WK, Leung MK, Lee TM, et al. Resting-state abnormalities in amnestic mild cognitive impairment: a meta-analysis. Transl Psychiatry 2016;6:e790.
[43] Xing XX, Zuo XN. The anatomy of reliability: a must read for future human brain mapping. Sci Bull 2018;63:1606–7.
[44] Zuo XN, Biswal BB, Poldrack RA. Editorial: reliability and reproducibility in functional connectomics. Front Neurosci 2019;13:117.
[45] Kublbock M, Woletz M, Hoflich A, et al. Stability of low-frequency fluctuation amplitudes in prolonged resting-state fMRI. Neuroimage 2014;103:249–57.
[46] Chen X, Lu B, Yan CG. Reproducibility of R-fMRI metrics on the impact of different strategies for multiple comparison correction and sample sizes. Hum Brain Mapp 2018;39:300–18.
[47] Zou Q, Miao X, Liu D, et al. Reliability comparison of spontaneous brain activities between BOLD and CBF contrasts in eyes-open and eyes-closed resting states. Neuroimage 2015;121:91–105.
[48] Zuo XN, Xing XX. Test-retest reliabilities of resting-state FMRI measurements in human brain functional connectomics: a systems neuroscience perspective. Neurosci Biobehav Rev 2014;45:100–18.
[49] Costafreda SG. Pooling FMRI data: meta-analysis, mega-analysis and multi-center studies. Front Neuroinform 2009;3:33.
[50] Xu K, Liu Y, Zhan Y, et al. BRANT: a versatile and extendable resting-state fMRI toolkit. Front Neuroinform 2018;12:52.
[51] Zhan Y, Ma J, Alexander-Bloch AF, et al. Longitudinal study of impaired intra- and inter-network brain connectivity in subjects at high risk for Alzheimer's disease. J Alzheimers Dis 2016;52:913–27.
[52] Zhan YF, Yao HX, Wang P, et al. Network-based statistic show aberrant functional connectivity in Alzheimer's disease. IEEE J Sel Top Signal Process 2016;10:1182–8.
[53] Power JD, Barnes KA, Snyder AZ, et al. Spurious but systematic correlations in functional connectivity MRI networks arise from subject motion. Neuroimage 2012;59:2142–54.
[54] Satterthwaite TD, Wolf DH, Loughead J, et al. Impact of in-scanner head motion on multiple measures of functional connectivity: relevance for studies of neurodevelopment in youth. Neuroimage 2012;60:623–32.
[55] Van Dijk KR, Sabuncu MR, Buckner RL. The influence of head motion on intrinsic functional connectivity MRI. Neuroimage 2012;59:431–8.
[56] Li T, Wang Q, Zhang J, et al. Brain-wide analysis of functional connectivity in first-episode and chronic stages of schizophrenia. Schizophr Bull 2017;43:436–48.
[57] Zaykin DV. Optimally weighted Z-test is a powerful method for combining probabilities in meta-analysis. J Evol Biol 2011;24:1836–41.
[58] Zhang J, Cheng W, Liu Z, et al. Neural, electrophysiological and anatomical basis of brain-network variability and its characteristic changes in mental disorders. Brain 2016;139:2307–21.
[59] Glahn DC, Laird AR, Ellison-Wright I, et al. Meta-analysis of gray matter anomalies in schizophrenia: application of anatomic likelihood estimation and network analysis. Biol Psychiatry 2008;64:774–81.
[60] Stouffer SA, Suchman EA, Evinney LC, et al. The American soldier: adjustment during Army life. (Studies in social psychology in World War II, Vol. I). Princeton, NJ: Princeton University Press; 1949.
[61] Hedges LV, Vevea JL. Fixed- and random-effects models in meta-analysis. Psychol Methods 1998;3:486–504.
[62] Beheshti I, Demirel H. Alzheimer's disease neuroimaging I. Feature-ranking-based Alzheimer's disease classification from structural MRI. Magn Reson Imaging 2016;34:252–63.
[63] Feng F, Wang P, Zhao K, et al. Radiomic features of hippocampal subregions in Alzheimer's disease and amnestic mild cognitive impairment. Front Aging Neurosci 2018;10:290.
[64] Abraham A, Milham MP, Di Martino A, et al. Deriving reproducible biomarkers from multi-site resting-state data: an autism-based example. Neuroimage 2017;147:736–45.
[65] Varoquaux G, Raamana PR, Engemann DA, et al. Assessing and tuning brain decoders: cross-validation, caveats, and guidelines. Neuroimage 2017;145:166–79.
[66] Nunes A, Schnack HG, Ching CRK, et al. Using structural MRI to identify bipolar disorders – 13 site machine learning study in 3020 individuals from the ENIGMA Bipolar Disorders Working Group. Mol Psychiatry 2018. https://doi.org/10.1038/s41380-018-0228-9.
[67] Rozycki M, Satterthwaite TD, Koutsouleris N, et al. Multisite machine learning analysis provides a robust structural imaging signature of schizophrenia detectable across diverse patient populations and within individuals. Schizophr Bull 2018;44:1035–44.
[68] Mutlu J, Landeau B, Gaubert M, et al. Distinct influence of specific versus global connectivity on the different Alzheimer's disease biomarkers. Brain 2017;140:3317–28.
[69] Bejanin A, La Joie R, Landeau B, et al. Distinct interplay between atrophy and hypometabolism in Alzheimer's versus semantic dementia. Cereb Cortex 2018;5:1889–99.
[70] Greicius MD, Srivastava G, Reiss AL, et al. Default-mode network activity distinguishes Alzheimer's disease from healthy aging: evidence from functional MRI. Proc Natl Acad Sci USA 2004;101:4637–42.
[71] Greicius MD, Kimmel DL. Neuroimaging insights into network-based neurodegeneration. Curr Opin Neurol 2012;25:727–34.
[72] Buckner RL, Sepulcre J, Talukdar T, et al. Cortical hubs revealed by intrinsic functional connectivity: mapping, assessment of stability, and relation to Alzheimer's disease. J Neurosci 2009;29:1860–73.
[73] Buckner RL, Andrews-Hanna JR, Schacter DL. The brain's default network: anatomy, function, and relevance to disease. Ann N Y Acad Sci 2008;1124:1–38.
[74] Raichle ME. The brain's default mode network. Annu Rev Neurosci 2015;38:433–47.
[75] Sorg C, Grothe MJ. The complex link between amyloid and neuronal dysfunction in Alzheimer's disease. Brain 2015;138:3472–5.
[76] Villain N, Fouquet M, Baron JC, et al. Sequential relationships between grey matter and white matter atrophy and brain metabolic abnormalities in early Alzheimer's disease. Brain 2010;133:3301–14.
[77] Shima K, Matsunari I, Samuraki M, et al. Posterior cingulate atrophy and metabolic decline in early stage Alzheimer's disease. Neurobiol Aging 2012;33:2006–17.
[78] Minoshima S, Giordani B, Berent S, et al. Metabolic reduction in the posterior cingulate cortex in very early Alzheimer's disease. Ann Neurol 1997;42:85–94.
[79] Grothe MJ, Teipel SJ. Alzheimer's disease neuroimaging I. Spatial patterns of atrophy, hypometabolism, and amyloid deposition in Alzheimer's disease correspond to dissociable functional brain networks. Hum Brain Mapp 2016;37:35–53.
[80] Pereira JB, Strandberg TO, Palmqvist S, et al. Amyloid network topology characterizes the progression of Alzheimer's Disease during the predementia stages. Cereb Cortex 2018;28:340–9.
[81] Wang WY, Yu JT, Liu Y, et al. Voxel-based meta-analysis of grey matter changes in Alzheimer's disease. Transl Neurodegener 2015;4:6.

[82] Yang J, Pan P, Song W, et al. Voxelwise meta-analysis of gray matter anomalies in Alzheimer's disease and mild cognitive impairment using anatomic likelihood estimation. J Neurol Sci 2012;316:21–9.
[83] Badhwar A, Tam A, Dansereau C, et al. Resting-state network dysfunction in Alzheimer's disease: a systematic review and meta-analysis. Alzheimers Dement (Amst). 2017;8:73–85.
[84] Zeidman P, Maguire EA. Anterior hippocampus: the anatomy of perception, imagination and episodic memory. Nat Rev Neurosci 2016;17:173–82.
[85] Bast T, Pezze M, McGarrity S. Cognitive deficits caused by prefrontal cortical and hippocampal neural disinhibition. Br J Pharmacol 2017;174:3211–25.
[86] Pasquini L, Scherr M, Tahmasian M, et al. Link between hippocampus' raised local and eased global intrinsic connectivity in AD. Alzheimers Dement 2015;11:475–84.
[87] Tahmasian M, Pasquini L, Scherr M, et al. The lower hippocampus global connectivity, the higher its local metabolism in Alzheimer disease. Neurology 2015;84:1956–63.
[88] Scheltens P, Blennow K, Breteler MMB, et al. Alzheimer's disease. The Lancet 2016;388:505–17.
[89] Nugent AC, Martinez A, D'Alfonso A, et al. The relationship between glucose metabolism, resting-state fMRI BOLD signal, and GABAA-binding potential: a preliminary study in healthy subjects and those with temporal lobe epilepsy. J Cereb Blood Flow Metab 2015;35:583–91.
[90] Marchitelli R, Aiello M, Cachia A, et al. Simultaneous resting-state FDG-PET/fMRI in Alzheimer disease: relationship between glucose metabolism and intrinsic activity. Neuroimage 2018;176:246–58.
[91] Abi-Dargham A, Horga G. The search for imaging biomarkers in psychiatric disorders. Nat Med 2016;22:1248–55.
[92] Bateman RJ, Xiong C, Benzinger TL, et al. Clinical and biomarker changes in dominantly inherited Alzheimer's disease. N Engl J Med 2012;367:795–804.
[93] Woo CW, Chang LJ, Lindquist MA, et al. Building better biomarkers: brain models in translational neuroimaging. Nat Neurosci 2017;20:365–77.
[94] Varoquaux G. Cross-validation failure: small sample sizes lead to large error bars. Neuroimage 2018;180:68–77.
[95] Salimi-Khorshidi G, Smith SM, Keltner JR, et al. Meta-analysis of neuroimaging data: a comparison of image-based and coordinate-based pooling of studies. Neuroimage 2009;45:810–23.
[96] Zhang Z, Liu Y, Jiang T, et al. Altered spontaneous activity in Alzheimer's disease and mild cognitive impairment revealed by regional homogeneity. Neuroimage 2012;59:1429–40.
[97] He X, Qin W, Liu Y, et al. Abnormal salience network in normal aging and in amnestic mild cognitive impairment and Alzheimer's disease. Hum Brain Mapp 2014;35:3446–64.
[98] Li Y, Wang X, Li Y, et al. Abnormal resting-state functional connectivity strength in mild cognitive impairment and its conversion to Alzheimer's disease. Neural Plast 2016;2016:4680972.
[99] Guo Y, Zhang Z, Zhou B, et al. Grey-matter volume as a potential feature for the classification of Alzheimer's disease and mild cognitive impairment: an exploratory study. Neurosci Bull 2014;30:477–89.
[100] Wang P, Zhou B, Yao H, et al. Aberrant intra- and inter-network connectivity architectures in Alzheimer's disease and mild cognitive impairment. Sci Rep 2015;5:14824.
[101] Li S, Yuan X, Pu F, et al. Abnormal changes of multidimensional surface features using multivariate pattern classification in amnestic mild cognitive impairment patients. J Neurosci 2014;34:10541–53.
[102] Jin D, Li A, Liu B, et al. Impaired whole brain functional connectivity in Alzheimer's disease: a multicenter study ($N = 688$). Singapore: Organization of Human Brain Mapping Annual Meeting 2018; 2018.
[103] Jin D, Xu J, Zhao K, et al. Attention-based 3D convolutional network for Alzheimer's disease diagnosis and biomarkers exploration. In: 2019 IEEE International Symposium on Biomedical Imaging (ISBI) 2019 April 8–11, 2019; Venice, Italy. p. 1047–51.
[104] Zhou HH, Singh V, Johnson SC, et al. Statistical tests and identifiability conditions for pooling and analyzing multisite datasets. Proc Natl Acad Sci USA 2018;115:1481–6.

Jiachen Li is currently a graduate student at the Department of Neurology, Xuanwu Hospital, Capital Medical University. Her research mainly focuses on the Alzheimer's disease using resting state functional magnetic resonance imaging.

Dan Jin is currently a graduate student at the Institute of Automation, Chinese Academy of Sciences and the University of Chinese Academy of Sciences. Her research mainly focuses on the brain network dysfunction and the computer-aided diagnosis of the Alzheimer's disease.

Yong Liu is a professor in Brainnetome Center, National Laboratory of Pattern Recognition, Institute of Automation, Chinese Academy of Sciences. He obtained his Ph.D. degree from Institute of Automation, Chinese Academy of Sciences (CASIA) in 2008. Since then, he joined CASIA as an assistant/associate research professor. He was a visiting scholar from April 2011 to March 2012 in Brain Mapping Unit in University of Cambridge. His present research is focused on the brain disorders with multimodal brain imaging.

Ying Han is a professor of Neurology at the Department of Neurology, Xuanwu Hospital, Capital Medical University. She is the PI of the multi-center study on subjective cognitive decline of preclinical Alzheimer's disease. Her research focuses on the prevention, diagnosis and intervention of Alzheimer's disease, especially the early diagnosis of Alzheimer's disease using multimodal neuroimaging techniques.